

## Dynamics of DNA during Pulsed-Field Gel Electrophoresis

Monica Olvera de la Cruz, Dilip Gersappe, and Edward O. Shaffer

Department of Materials Science and Engineering, Northwestern University, Evanston Illinois 60208

(Received 28 July 1989)

We study polymer pulsed-field gel electrophoresis by an off-lattice computer simulation. The effects of  $90^\circ$  rotations of the field on the chains' conformations are analyzed. We find that  $90^\circ$  pulsed fields can be used to increase significantly the resolution of the chains' separation according to size.

PACS numbers: 82.45.+z, 87.22.Fy

Gel electrophoresis is a technique widely used in modern molecular biology to separate proteins and nucleic acids according to size. At constant electric fields, however, the technique is unable to separate long DNA molecules. Pulsed-field techniques<sup>1-3</sup> based on empirical observations have been developed to separate long chains. Great advances towards the understanding of the chain dynamics during gel electrophoresis have been recently made by computer simulations.<sup>4-8</sup>

A long polymer chain diffusing through a network of fixed obstacles in the presence of an electric field undergoes molecular-weight-dependent cyclic changes from expanded to contracted conformations.<sup>5-8</sup> The mobility, on the other hand, loses its molecular-weight dependence as the chain size and/or the electric field increase. It plateaus to a constant value, resulting in the inability to separate long chains.

The molecular-weight dependence of the chains' modes of oscillations can be used to optimize the separation process. Pulsed-field gel electrophoresis (PFGE) with switching angles of  $180^\circ < \Theta < 90^\circ$ , for example, has shown to increase the resolution of the separation technique.<sup>1</sup> In this paper we study the separation of long chains according to size by orthogonal PFGE. We describe the effect of  $90^\circ$  rotations on the chain conformations as a function of field strength and molecular weight. We find that when perpendicular fields are used the chains can be prevented from contracting; they can be kept in open U conformations, in agreement with the microscope observations of Schwartz and Koval.<sup>2</sup> We analyze the mobility as a function of chain length and pulse time. We find that the chain dynamics cannot be described by the tube reptation models<sup>9</sup> of gel electrophoresis even at small electric fields.

In the reptation model<sup>10</sup> an ideal chain of  $N$  units of length  $l$  in a gel is confined to diffuse along the path of a tube whose diameter is the average distance  $a$  between gel points. The tube is constructed following the chain conformation in the gel which is known by statistical mechanics. Therefore, in the absence of a driving force, leaking of the chain through the gel junction points is not allowed due to the entropic barriers associated with these fluctuations.

Various groups have extended the tube-model concepts

to describe gel electrophoresis.<sup>9</sup> They postulate the chain statistics in the steady state, assuming that in the presence of a field leaking is also forbidden. The dynamics are, therefore, determined by the end leading segment, which in the presence of a field  $E$ , is biased in the field direction, giving rise to an average orientation. The mobility is then predicted to lose its molecular-weight dependence as  $NE^2$  increases.<sup>7</sup> At high electric fields these assumptions are wrong, as a stretched chain undergoes fluctuations that entangle it back in the gel.<sup>4,5,7</sup> Even in the presence of a small field, leaking is an important factor determining the chain dynamics.<sup>6</sup> The breakdown of the tube models is more apparent when pulsed fields are used.<sup>8</sup>

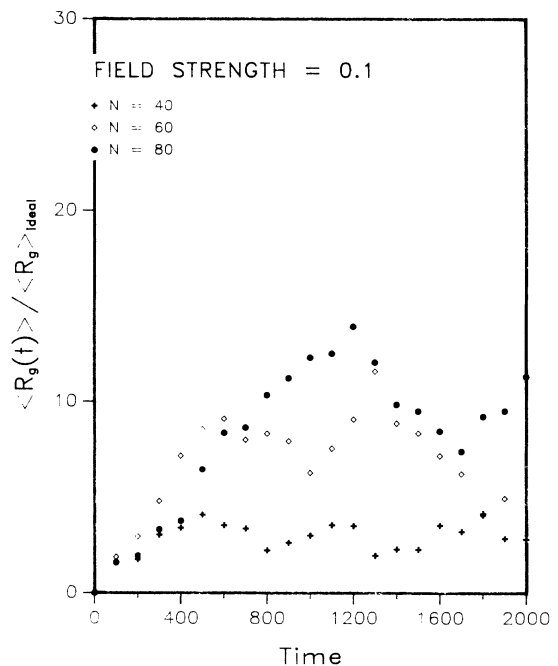


FIG. 1. The average radius of gyration  $\langle R_g \rangle$  scaled by the unperturbed value  $\langle R_g \rangle_{ideal}$  vs time for different chain lengths  $N$  at constant electric field  $E_s = 0.1$ .  $\langle R_g \rangle_{ideal}$  is the average radius of gyration in the absence of an electric field. Each point in the figure corresponds to an average over ten realizations of the process all with different initial Gaussian configuration.

In order to simulate gel electrophoresis a continuous model which includes the internal degrees of freedom of the chain between gel points is required. We used a two-dimensional off-lattice computer simulation to solve the Langevin equation of motion. In the simulation the diffusion of the chains is restricted by a periodic array of obstacles that represents the gel junction points. The chain has  $N$  beads and  $N-1$  springs, each of charge  $q$ . The root mean square of the spring length is  $l$ . The Langevin equation of motion, described in detail elsewhere,<sup>6</sup> includes a thermal force  $\eta$ , a viscous drag, entropic spring forces, and the applied field force,

$$\partial \mathbf{r}_i(t) / \partial t = \boldsymbol{\eta}_i(t) + 2D \{ \mathbf{r}_{i+1}(t) + \mathbf{r}_{i-1}(t) - 2\mathbf{r}_i(t) \} + \mathbf{E}_s D,$$

where  $\mathbf{r}_i(t)$  is the position of the  $i$ th bead,  $D$  is the diffusion coefficient of the bead, and

$$\langle \boldsymbol{\eta}_i(t) \rangle = 0,$$

$$\langle \boldsymbol{\eta}_i(t) \otimes \boldsymbol{\eta}_j(t') \rangle = 2D\delta(t-t')\delta_{ij} \mathbf{1},$$

where  $\mathbf{1}$  is the unit matrix. In the simulation we used a scaled field  $E_s = qEl/k_B T$  and the gel spacing is  $2l$ . The dynamics are set by small time iterations such that a

continuous diffusive drift is simulated.<sup>6</sup> At each iteration all beads are moved in the order of a random permutation from 1 to  $N$  and according to forces dictated by the equation of motion, rejecting the moves that cross the gel.<sup>11</sup>

In Fig. 1 we show the average chain radius of gyration as time evolves under a constant electric field  $E_s = 0.1$ . The mobility in this case is molecular-weight and field-strength independent.<sup>6</sup> A chain stretches when regions higher in monomer concentration (formed by leaking) pull the rest of the chain, bringing the chain end segments close together. Closed J (hooks) and U-shaped conformations result [Fig. 2(a)]. When the net electric force decreases, the denser regions tend to form towards the chain ends, resulting in more open and shorter J chain conformations [Fig. 2(c)]. The hooked chain is pulled by the leading segment which collides with the gel, increasing the concentration of monomers around it. When a new dense region is formed, this process is repeated, leading to the oscillations shown in Fig. 1. Our results agree qualitatively with other simulations.<sup>5,8</sup>

We examine the effects of rotating the electric field  $90^\circ$  in the chain conformation. If the field is rotated

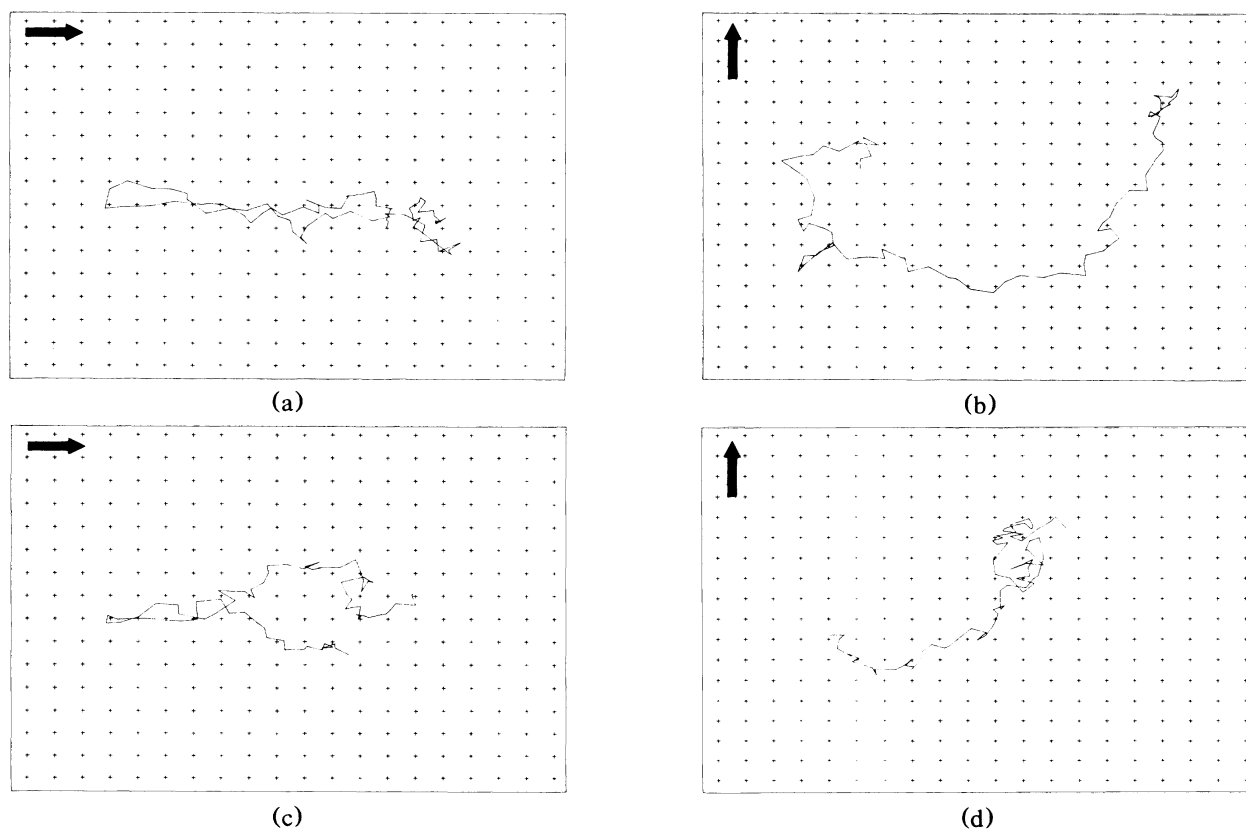


FIG. 2. The chain conformation during gel electrophoresis. The arrows indicate the direction of the electric field; (a),(b) and (c),(d) correspond to  $E_s = 0.15$  and  $E_s = 0.1$ , respectively. In both sequences  $N = 80$ . The snapshots (a) and (c) are taken at 800 time steps with the chain starting in a random coil configuration. The snapshots (b) and (d) show the conformations at 400 time steps after the rotation of the field by  $90^\circ$  [the starting configurations were those of (a) and (c), respectively].

when the chain is in the hooked J or nearly U conformation, the chain is pulled by the denser end segment, increasing the component of the end-to-end vector perpendicular to the new field direction, resulting in very open U conformations [Fig. 2(b)]. On the other hand, if the field is rotated while dense monomer regions are present around the middle part of the chain, leaking occurs, resulting in coiled-up conformations.

At smaller electric fields, the mechanism by which the chain migrates is also governed by the starting conformation of the chain. If the field is rotated when the chain is almost free of dense regions, instabilities can form along the chain. When they are sufficiently near the ends, they pull the end segments and leak through the entanglements [Fig. 2(d)]. Meanwhile, if the field is rotated when dense regions are concentrated near the ends of the chain, the end that is more dense is the one that pulls the chain, forming open U shapes.

Our simulation shows that perpendicular pulsed-field rotations prevent the collapse of the chain and give rise to open U conformations (Fig. 2), as shown experimentally.<sup>2</sup> Since the larger the chain, the longer the cycle from stretched to contracted conformations (Fig. 1), for a given chain length there is an optimum switching time between rotations to prevent the collapse of the chain. If the switching time is much shorter than the stretching time of the chain (the case of longer chains for a fixed pulsed rate), leaking can occur when the chain aligns along the new field direction. The changes in conformations during pulsed-field rotations as a function of molecular weight can be used to separate the chains according

to size.

In Fig. 3 we show the center of mass as a function of time during orthogonal PFGE. The switching time  $\tau_s = 800$  and  $E_s = 0.1$  in both directions. For  $E_s = 0.1$  the chain mobility for  $N \geq 40$  at constant-field gel electrophoresis is the saturation value  $\mu_s$ . For a gel spacing of  $2l$ , the mobility at constant fields saturates to the constant value<sup>6</sup>  $\mu_s = 0.25\mu_0$ , where  $\mu_0$  is the mobility of a free chain [that is, when there is no gel, in which case the mobility  $\mu_0$  is independent of  $N$  and  $E$  (Refs. 4 and 7)]. When  $90^\circ$  pulsed fields are used we find that the mobility along the  $x$  direction  $\mu^x$  is roughly  $\mu_s/2$  for  $N = 40$ . Meanwhile  $\mu^x$  is approximately  $\mu_s/4$  for  $N = 60$  and 100. Figure 1 shows that after  $t = 800$ , chains of  $N \leq 40$  have at least completed one cycle of stretched-to-contracted conformations so one would expect  $\mu^x$  to be half the mobility at constant field. As longer chains have longer cycles, the orientation effects during pulsed fields cause a higher reduction in  $\mu^x$ . The saturation of  $\mu^x$  for long chains leads to a window of molecular weights for which the resolution is optimum for a fixed pulse rate, in agreement with experiments. If the pulse time is reduced to 100, keeping  $E_s = 0.1$  in both directions, no increase in the resolution of separation is observed (Fig. 4), as the pulse time in this case is much smaller than the stretching time of the chains. For  $\tau_s = 100$  we find that  $\mu^x$  is roughly  $\mu_s/3$  for  $N \geq 40$ , revealing a minimum in the mobility versus pulse time for long chains (compare Figs. 3 and 4).

Our simulation explains how pulsed-field rotation methods separate the chains according to size. We find a

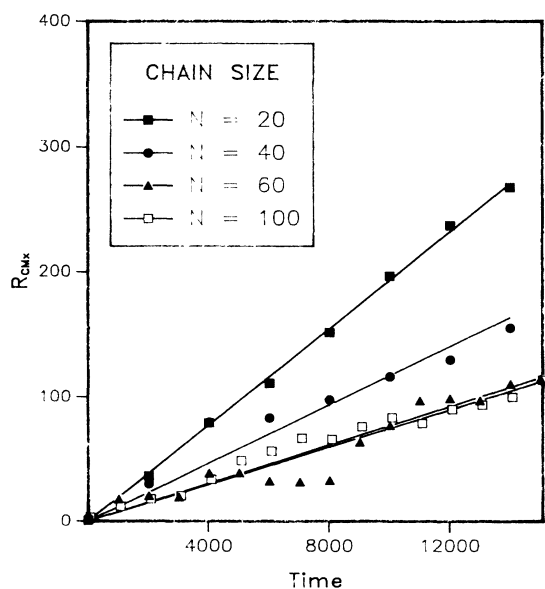


FIG. 3. The center of mass  $R_{c.m.x}$  vs time during orthogonal pulsed fields for chains of  $N = 20, 40, 60,$  and  $100$ . The pulse rate between  $x$  and  $y$  directions is  $800$  and  $E_s = 0.1$  along both directions.

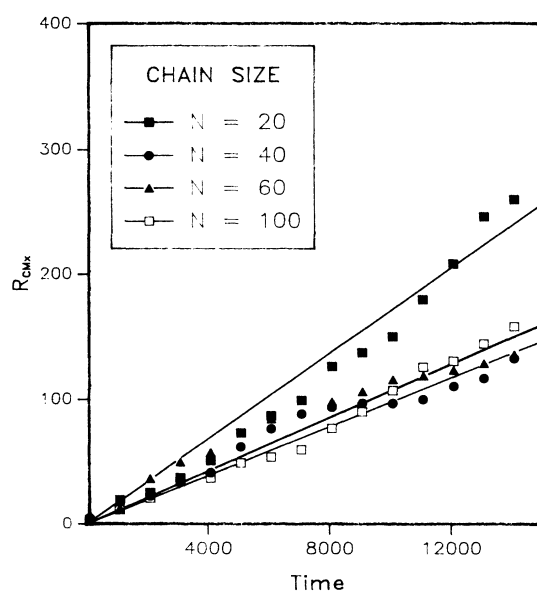


FIG. 4. The center of mass  $R_{c.m.x}$  vs time during orthogonal pulsed fields for chains of  $N = 20, 40, 60,$  and  $100$ . The pulse rate between  $x$  and  $y$  directions is  $100$  and  $E_s = 0.1$  along both directions.

window of resolution of molecular sizes as a function of pulse time. The mechanism of orientation during orthogonal PFGE is more complicated than what simplified theories using the reptation model would lead us to believe. Our conclusion applies to small fields widely used experimentally for pulsed-field separation techniques, for example, those used in Ref. 2.

This work was supported by the National Institutes of Health. The computation was done on the Cray X-MP Computer at the National Center for Supercomputer Applications. We thank A. Mondragon and J. M. Deutsch for useful discussions. M. Olvera de la Cruz thanks the David and Lucile Packard Foundation and the donors of the Petroleum Research Fund for partial financial support.

---

<sup>1</sup>D. C. Schwartz and C. R. Cantor, *Cell* **37**, 67 (1984).

<sup>2</sup>D. C. Schwartz and M. Koval, *Nature (London)* **338**, 520 (1989).

<sup>3</sup>G. F. Carle, M. Frank, and M. V. Olson, *Science* **232**, 65

(1986).

<sup>4</sup>M. Olvera de la Cruz, J. M. Deutsch, and S. F. Edwards, *Phys. Rev. A* **33**, 2047 (1986).

<sup>5</sup>J. M. Deutsch, *Science* **240**, 922 (1988).

<sup>6</sup>E. O. Shaffer and M. Olvera de la Cruz, *Macromolecules* **22**, 1351 (1989); E. O. Shaffer, thesis, Northwestern University, 1988 (unpublished).

<sup>7</sup>M. Olvera de la Cruz, thesis, Cambridge University, 1984 (unpublished).

<sup>8</sup>B. H. Zimm, *Phys. Rev. Lett.* **61**, 2965 (1988); T. A. J. Duke, *Phys. Rev. Lett.* **62**, 2877 (1989); J. M. Deutsch and T. L. Madden, *J. Chem. Phys.* **90**, 2476 (1989).

<sup>9</sup>L. S. Lerman and H. L. Frisch, *Biopolymers* **21**, 995 (1982); O. J. Lumpkin and B. H. Zimm, *Biopolymers* **21**, 2315 (1982); C. P. Bean and H. Herve, *Biophys. J.* **41**, A289 (1983); O. J. Lumpkin, P. Dejardin, and B. H. Zimm, *Biopolymers* **24**, 1575 (1985); G. W. Slater and J. Noolandi, *Biopolymers* **24**, 2181 (1985).

<sup>10</sup>P. G. de Gennes, *J. Chem. Phys.* **55**, 572 (1971).

<sup>11</sup>When the rejection ratio is high the model leads to metastability. The metastability introduced by the Monte Carlo technique is discussed in Ref. 4 for lattice model simulations. In our off-lattice Langevin approach we checked that no metastability was introduced for the field strengths used here (Ref. 6).